

## **Lateral Vehicle Following in a Cooperative Vehicle Platooning Application An $H_\infty$ approach**

Van Den Berg, Daniel; Van Der Ploeg, Chris; Alirezaei, Mohsen; Van De Wouw, Nathan

**DOI**

[10.23919/ECC54610.2021.9655008](https://doi.org/10.23919/ECC54610.2021.9655008)

**Publication date**

2021

**Document Version**

Accepted author manuscript

**Published in**

Proceedings of the European Control Conference, ECC 2021

**Citation (APA)**

Van Den Berg, D., Van Der Ploeg, C., Alirezaei, M., & Van De Wouw, N. (2021). Lateral Vehicle Following in a Cooperative Vehicle Platooning Application: An  $H_\infty$  approach. In *Proceedings of the European Control Conference, ECC 2021* (pp. 1802-1807). IEEE. <https://doi.org/10.23919/ECC54610.2021.9655008>

**Important note**

To cite this publication, please use the final published version (if applicable).  
Please check the document version above.

**Copyright**

Other than for strictly personal use, it is not permitted to download, forward or distribute the text or part of it, without the consent of the author(s) and/or copyright holder(s), unless the work is under an open content license such as Creative Commons.

**Takedown policy**

Please contact us and provide details if you believe this document breaches copyrights.  
We will remove access to the work immediately and investigate your claim.

# Lateral Vehicle Following in a Cooperative Vehicle Platooning

## Application: an $\mathcal{H}_\infty$ approach

Daniel van den Berg<sup>1</sup>, Chris van der Ploeg<sup>2,4</sup>, Mohsen Alirezaei<sup>3,4</sup>, Nathan van de Wouw<sup>4</sup>

**Abstract**—Lateral control in the absence of lane markings is an essential safety fallback for an autonomous vehicle in cooperative driving applications. Point following control is one such solutions for lateral control. However, it suffers from corner cutting and severe disturbance amplification throughout the platoon. In this paper, a new model for controller synthesis is proposed which supports including the error induced by the road curvature in the communication between two vehicles. This enables the trailing vehicle to deduce the actual road error states, which negates steady-state corner cutting if these errors are controlled to zero. To demonstrate the benefits of this new control model, an  $\mathcal{H}_\infty$  control framework is used to design a lateral controller which minimizes the lateral overshoot of the vehicles during transient maneuvering. The proposed approach has been evaluated using numerical simulations. Simulation results show that the lateral overshoot can be reduced by a factor 10 with respect to existing lateral control solutions.

### I. INTRODUCTION

Road usage in the Netherlands keeps on increasing and since 2014 the length of traffic jams has trended upwards [1, 2]. With advances in vehicle technologies, platooning is becoming a more realistic solution to various traffic-related challenges, such as the aforementioned traffic jams [3]. Platooning technology allows the traffic to be more tightly packed, increasing road usage efficiency and is an effective way to reduce fuel consumption [4]. In the context of platooning, lateral control of a platoon member in the absence of lane-markings is essential for further alleviation of driver tasks. Short driving distances in a typical platooning application could result in an obstructed view of the lanes observed by in-vehicle cameras. Moreover, in particular emergency situations (e.g., due to a road-blockage) it is essential to apply a "follow-the-leader" concept by following the manually steered leader-vehicle of the platoon.

Different approaches can be used for lateral control, such as path following or single point following [5]. With path following, the path is reconstructed using both information from the preceding vehicle as well as visual identification of road markings. However, sensor noise and short following

distances between two vehicles degrade reliability and accuracy of the reconstructed path. The single point following approach only needs to track a single point, defined within its field of view. This information can be more reliably measured and does not require the continuity of a path, which would be needed in path-following. However, this approach does suffer from the phenomenon of corner cutting when driving in tight radius corners [6]. Several methods exist to counteract this corner cutting, see for example [7, 8]. However, in contrast to the work presented in this paper these methods are applied in the context of lane-following or lane-keeping without consideration for string-stability.

The main contribution of this paper is a single point following method that mitigates corner cutting and can be used within the context of vehicle platooning without the need for information on the path of the preceding vehicle. In addition, an intuitive control design method using  $\mathcal{H}_\infty$  optimization is proposed. It allows the user to actively trade-off between tracking performance and minimization of disturbance propagation throughout the platoon.

The paper is organized as follows. Section II covers the vehicle platoon model and presents the proposed point following method. Section III covers preliminaries on the notion of lateral string stability, required for insights used in synthesis of the  $\mathcal{H}_\infty$ -controller provided in Section IV. Section V will cover the simulation results. Section VI will provide a conclusion to the work presented.

### II. PROBLEM FORMULATION

The main control objective of this work is to have a trailing vehicle track the lateral movement of a preceding vehicle without steady-state error. A secondary requirement in the design of a platooning system is the mitigation of disturbance amplification over the platoon. This phenomenon is covered by the notion of string stability, which will be covered in Section III.

#### A. Vehicle Platoon Model

Fig. 1 depicts two vehicles in a platoon of length  $n$ , with the lead vehicle either manually driven or employing lane-keeping control without error. We assume that each of the vehicles in the platoon can communicate with its nearest following vehicle. Moreover, it is assumed that this communication is free of delay and noise. Finally, it is assumed that the platoon is homogeneous, meaning that each of the vehicles in the platoon has identical input-output dynamics and the controller used in the following vehicles is identical.

<sup>1</sup>Daniel van den Berg is with the Delft Centre for Systems and Control, TU Delft, 2628 CD, Delft, The Netherlands D.G.vandenBerg@tudelft.nl

<sup>2</sup>Chris van der Ploeg is with the Department of Integrated Vehicle Safety, TNO, 5708 JZ, Helmond, The Netherlands

<sup>3</sup>Mohsen Alirezaei is with Siemens Digital Industries Software, 5708 JZ, Helmond, The Netherlands

<sup>4</sup>Nathan van de Wouw, Mohsen Alirezaei and Chris van der Ploeg are with the Department of Mechanical Engineering, TU Eindhoven, 5600 MB, Eindhoven, The Netherlands. Nathan van de Wouw is also with University of Minnesota, Department of Civil, Environmental and Geo-Engineering, Minneapolis, MN, USA

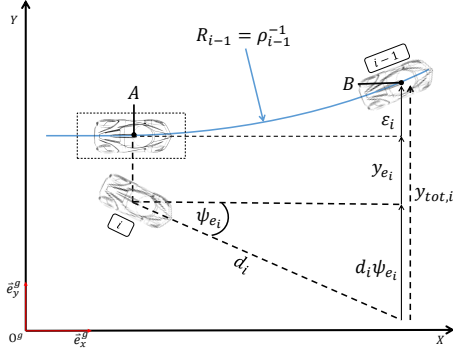


Fig. 1. Depiction of two vehicles in a lateral platoon with the definition of the variables for lateral control in platooning.

Fig. 1 shows the definition of the variables used in lateral control. When vehicle  $i$  has access to path information, it is capable of deducing both errors  $y_{e,i}$ , the lateral offset error, and the heading error  $\psi_{e,i}$ . For  $y_{e,i} = \psi_{e,i} = 0$ , the trailing vehicle is at the desired location and driving with the desired heading. Errors  $y_{e,i}$  and  $\psi_{e,i}$  can be written as functions of the lateral vehicle dynamics of vehicle  $i$  and  $i-1$ . In [9], a state-space description incorporating the dynamics of the vehicle's steering system of the following form can be found:

$$\dot{x}_i = A_i x_i + B_i \delta_{i,ref} + E_i \dot{\theta}_{s,i-1}, \quad (1)$$

where the state vector is defined as  $x_i = [v_{y,i} \ \dot{\psi}_i \ y_{e,i} \ \psi_{e,i} \ \delta_i \ \dot{\delta}_i]^T$  with  $v_{y,i}$  the lateral velocity,  $\dot{\psi}_i$  the yaw rate,  $\delta_i$  the steering wheel angle and  $\dot{\delta}_i$  the rate of change for the steering wheel angle.  $\delta_{i,ref}$  is the control input and  $\dot{\theta}_{s,i-1}$  the change in curvature over time of the path that needs to be tracked. The longitudinal velocity  $v_x$  is assumed to be constant across the platoon. The steering dynamics are described by a second-order system of the form [10]:

$$\ddot{\delta}_i = -2\zeta\omega_n\dot{\delta}_i + \omega_n^2(\delta_{ref,i} - \delta_i). \quad (2)$$

In (2),  $\zeta$  represents the damping ratio of the steering actuator,  $\omega_n$  its natural frequency and  $\delta_{ref,i}$  the steering wheel reference.

### B. Point Following Control

It is assumed that each vehicle in the platoon is equipped with a camera, capable of measuring the distance  $y_{tot,i}$ . This can be done by comparing the Euclidean distance from its own location over a distance  $d_i$  (the look-ahead distance [11]) to the point the vehicle is tracking. If this tracking point is defined to be on the back of the preceding vehicle it can be used as a vehicle following solution. This measurement is defined as  $y_{tot,i}$ :

$$y_{tot,i} = \varepsilon_i + y_{e,i} + d_i \psi_{e,i}, \quad (3)$$

where  $\varepsilon_i$  is the distance error due to the road curvature.

### C. The Road Error Measurement

The measurement (3) is partially a linear combination of  $y_{e,i}$  and  $\psi_{e,i}$ . Vehicle  $i$  is capable of accessing each state individually when having knowledge of the distance  $\varepsilon_i$ . This knowledge can be provided by vehicle  $i-1$  by means of logging its location over a short period of time.

To elaborate on this, consider the path vehicle  $i-1$  travels from point A in Fig. 1, to where vehicle  $i-1$  currently is, denoted by point B. The time it takes vehicle  $i-1$  to travel this path is given by  $t_{la} \approx d_i v_x^{-1}$ . The lateral displacement of vehicle  $i-1$  when travelling from point A to B in time  $t_{la}$  is calculated by integrating its *global*  $Y$  velocity,  $\dot{Y}$ , over a time interval of travel length  $t_{la}$ . Velocity  $\dot{Y}$  can be expressed in the local vehicle velocities as

$$\dot{Y} = v_x \sin(\psi_{i-1}(t)) + v_{y,i-1}(t) \cos(\psi_{i-1}(t)).$$

Hence, the global  $Y$  displacement,  $\Delta Y$ , can be calculated as

$$\Delta Y = \int_{t-t_{la}}^t v_x \sin(\psi_{i-1}(t)) + v_{y,i-1}(t) \cos(\psi_{i-1}(t)) dt.$$

The calculation of  $\Delta Y$  can be simplified by assuming that, during highway driving,  $v_x \gg v_{y,i-1}(t)$ . This removes the necessity to have information on  $v_{y,i-1}(t)$ , information which is often difficult to practically obtain. Equation 4 can then be further simplified as

$$\Delta Y \approx v_x \int_{t-t_{la}}^t \sin(\psi_{i-1}(t)) dt. \quad (4)$$

The yaw angle  $\psi_{i-1}$  in (4) can be calculated using the on-board yaw-rate measurement of vehicle  $i-1$  and integrating it over the time period  $t_{la}$ . In the situation depicted in Fig. 1, the lateral displacement  $\Delta Y$  is equal to the distance  $\varepsilon_i$ . By performing this integration over short periods of time vehicle  $i-1$  can provide vehicle  $i$  information on the value of  $\varepsilon_i$  contained with the  $y_{tot,i}$  measurement. With access to  $\varepsilon_i$ , (3) can be used to construct the lateral error  $e_i$ :

$$e_i = y_{tot,i} - \varepsilon_i = y_{e,i} + d_i \psi_{e,i}, \quad (5)$$

which provides access to an error definition based on a linear combination of the state space states  $y_{e,i}$  and  $\psi_{e,i}$ . This result opens the possibility to access the states  $y_{e,i}$  and  $\psi_{e,i}$  individually.

### D. Estimation of Individual Errors

Further information from the error measurement in (5) can be obtained by decoupling it into the individual errors  $y_{e,i}$  and  $\psi_{e,i}$  using an observer. By choosing the output matrix as  $C = [0 \ 0 \ 1 \ d_i \ 0 \ 0]$  for the state-space system in (1), the system is rendered observable. By designing, for example, a Luenberger type observer for vehicle  $i$ , the desired states  $y_{e,i}$  and  $\psi_{e,i}$  can be asymptotically reconstructed based on the error measurement  $e_i = y_{e,i} + d_i \psi_{e,i}$ . The observer can be viewed independent of the control design using the separation principle. Throughout the remainder of the paper, it is assumed that the measurements  $y_{e,i}$  and  $\psi_{e,i}$  are available for control design, using some form of linear observer with sufficiently fast error dynamics.

### E. Control Objectives

The main objective of the controller is to laterally track the preceding vehicle whilst keeping the disturbance propagation minimal, i.e., to strive for string stability. From a practical perspective, the desire for having string stability is safety related. If each of the vehicles in the platoon increasingly violates the desired lateral position of the preceding vehicle then at a certain point in time it could lead to potentially harmful consequences. With a limited number of vehicles in the platoon, a small amount of disturbance amplification can be rendered safe. Such a safety bound has to be determined by the designer and the use case for which the controller is designed (this should be done in the scope of functional safety of such an automated system according to the ISO26262 norm [12]). The control objectives can be summarized as follows:

- Asymptotic zeroing of the lateral vehicle following errors for a constant external input:

$$\lim_{t \rightarrow \infty} y_{e,i}(t) = 0,$$

$$\lim_{t \rightarrow \infty} \psi_{e,i}(t) = 0,$$

- Minimize the lateral overshoot.
- The settling time of the transient following response needs to be fast enough such that the path tracking objectives are met within a designed time.
- The controllers should generate a reference command such that a vehicle is physically capable of following it, i.e. the controllers are constrained by the hardware available on the vehicles.

### III. STRING STABILITY

In [3], a string stability definition based on linear system theory is presented. Although originally developed for longitudinal platooning, it is equally suited for the lateral platooning problem. In general, a connected string of  $m$  systems can be represented by the following lumped state-space system:

$$\begin{bmatrix} \dot{x}_0 \\ \dot{x}_1 \\ \vdots \\ \dot{x}_m \end{bmatrix} = \begin{bmatrix} A_r & & O \\ A_1 & A_0 & \\ & \ddots & \ddots \\ O & & A_1 & A_0 \end{bmatrix} \begin{bmatrix} x_0 \\ x_1 \\ \vdots \\ x_m \end{bmatrix} + \begin{bmatrix} B_r \\ 0 \\ \vdots \\ 0 \end{bmatrix} u_r. \quad (6)$$

The matrices  $A_r$  and  $A_0$  denote the dynamics of the host vehicle and trailing vehicles, respectively. The matrix  $A_1$  describes how a change in dynamics of the preceding vehicle influences the states of the trailing vehicle. The matrix  $B_r$  is the input matrix for the host vehicle. Because of the homogeneity assumption, the vehicle states are allowed to be lumped together into a single state vector as  $x = [x_0^T \ x_1^T \ \dots \ x_m^T]^T$  such that (6) can be written as

$$\dot{x} = Ax + Bu_r. \quad (7)$$

When we express the output  $y_i$  of vehicle  $i$  as

$$y_i = C_i x, \quad (8)$$

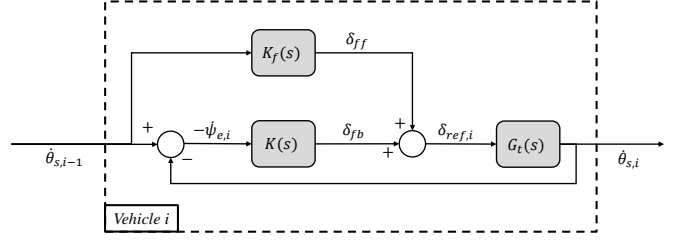


Fig. 2. Block scheme of a vehicle in the platoon.

it is possible to express the input-output behaviour of the model in (7) and (8) as a transfer function. This transfer function describes how the external input  $u_r$  translates to an output  $y_i$  for vehicle  $i$

$$y_i(s) = P_i(s)u_r(s) + O_i(s)x(0), \quad (9)$$

where  $P_i(s) = C_i(sI - A)^{-1}B$  is the transfer function from external input to chosen output and  $O_i = C_i(sI - A)^{-1}$  the transfer function from any initial condition error to the chosen output. In similar fashion we can write output  $y_{i-1}(s)$  (with  $x(0) = 0$ ) as

$$y_{i-1}(s) = P_{i-1}(s)u_r(s), \quad (10)$$

From (10) external input  $u_r(s)$  can also be written as

$$u_r(s) = P_{i-1}^{-1}(s)y_{i-1}(s). \quad (11)$$

Combining (9) and (11) a transfer function linking the outputs  $y_{i-1}(s)$  and  $y_i(s)$  can be found

$$y_i(s) = P_i(s)P_{i-1}^{-1}(s)y_{i-1}(s) =: \Gamma_i(s)y_{i-1}(s), \quad (12)$$

where  $\Gamma_i(s)$  represents the string stability complementary sensitivity. Since  $\Gamma_i(s)$  is a linear transfer function, string stability can be defined using a system norm. From [3], a platoon is considered strictly string stable if and only if

$$\|P_1(s)\|_\infty < \infty \quad (13)$$

$$\|\Gamma_i(s)\|_\infty \leq 1 \quad \forall i \in \mathbb{N} \setminus \{1\}. \quad (14)$$

Here,  $P_1(s)$  is the transfer function of the host vehicle, and the norm bound indicates that the dynamics of the first vehicle should be stable. The second requirement (14) states that if the  $\mathcal{H}_\infty$  norm of  $\Gamma_i(s)$  is upper-bounded by 1, vehicle  $i$  will have no amplification of output  $y_{i-1}$  in its output  $y_i$ .

#### A. Lateral String Stability

Fig. 2 shows the block scheme of a single vehicle in the platoon. Transfer function  $G_t(s)$  is the transfer function of steering input to output  $\theta_{s,i}$ . Furthermore, the errors  $\psi_{e,i}$  and  $y_{e,i}$  can be written as follows [9]:

$$\psi_{e,i} = \frac{1}{s}\dot{\psi}_{e,i} = \frac{1}{s}(\dot{\theta}_{s,i} - \dot{\theta}_{s,i-1}), \quad (15a)$$

$$y_{e,i} = \frac{v_x}{s^2}\dot{\psi}_{e,i} = \frac{v_x}{s^2}(\dot{\theta}_{s,i} - \dot{\theta}_{s,i-1}). \quad (15b)$$

The feedback controller  $K(s)$  in Fig. 2 contains the two feedback controllers and is further expanded in Fig. 3. Herein,  $K_{y_e}(s)$  and  $K_{\psi_e}(s)$  are the individual feedback controllers to be designed.  $K_f(s)$  in Fig. 2 contains the feedforward controller.

By tracing the path from  $\dot{\theta}_{s,i}$  to  $\dot{\theta}_{s,i-1}$ , the transfer function for assessing lateral string stability can be found as

$$\Gamma_i = \frac{G_t K_f + G_t K}{1 + G_t K} = \frac{G_t K_f}{1 + G_t K} + \frac{G_t K}{1 + G_t K}. \quad (16)$$

#### IV. CONTROLLER DESIGN

The definition on the string stability requirement motivates the development of an  $\mathcal{H}_\infty$  optimization-based controller synthesis approach. The goal for the controller is to minimize the disturbance amplification and vehicle-following errors while providing internal stability. A two-degree-of-freedom controller will be designed using the Robust Control toolbox in MATLAB [13], comprising a feedforward and feedback controller. The feedback controller consists of two individual feedback controllers, one for each road error state, see Fig. 3.

Fig. 4 shows the generalized plant with its exogenous inputs and outputs, representing a controlled vehicle in the platoon. It is assumed that no exogenous disturbances are present in the system. Included in the generalized plant are three weights. Weight  $W_u$  penalizes the control action and can be used to limit controller action. Weight  $W_T$  penalizes the (string stability) complementary sensitivity function, and can be used to weight the system performance in terms of the amplification of disturbances along the platoon. Finally, weight  $W_e$  penalizes the error signal and can be used to regulate the steady-state error and is given by and is given by

$$W_e = \begin{bmatrix} W_{e1,1} & 0 \\ 0 & W_{e2,2} \end{bmatrix},$$

with  $W_{e1,1}$  and  $W_{e2,2}$  to be designed. The weights in Fig. 4 can be used to shape the performance of the system. For this purpose each output  $z_j, \forall j$ , is first written as a function of exogenous input  $\dot{\theta}_{s,i-1}$ . Output  $z_1$  can be written as

$$z_1 = W_e \underbrace{(I + EG_t K_{fb})^{-1} (E - EG_t K_f)}_{Z_1(s)} \dot{\theta}_{s,i-1}, \quad (17)$$

where

$$K_{fb} = \begin{bmatrix} K_{\psi_{e,i}} & K_{y_{e,i}} \end{bmatrix}.$$

Output  $z_2$  can be written as

$$z_2 = W_T \Gamma_i \dot{\theta}_{s,i-1}, \quad (18)$$

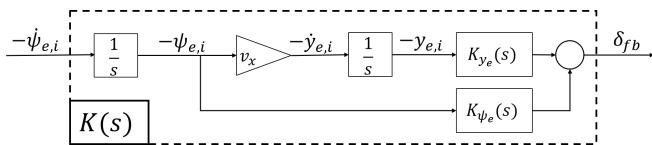


Fig. 3. Control block  $K(s)$  expanded.

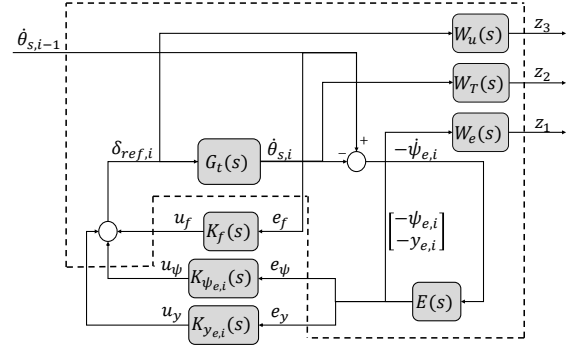


Fig. 4. Generalized plant used for controller synthesis.

with  $\Gamma_i$  as in (16). Finally, performance signal  $z_3$  can be written as

$$z_3 = W_u \underbrace{(1 + K_{fb} E G_t)^{-1} (K_f + K_{fb} E)}_{Z_3(s)} \dot{\theta}_{s,i-1}. \quad (19)$$

With these transfer functions it is now possible to design the weights accordingly, as detailed below.

##### A. Weight $W_T(s)$

Representative steering behaviour for a highway lane change can be approximated as a sinusoidal input on the steering wheel. Typical frequencies for such an input are around 0.1 Hz [14]. Within this frequency range, steady-state path tracking is desired. Based on the string stability requirement in (14) and the desire to have minimal disturbance propagation, the weight  $W_T$  is designed such that it has a gain of 0 dB up to a bandwidth of 0.1 Hz. The gain of the string stability complementary sensitivity for higher frequencies is disregarded for the scope of vehicle following. The weight on  $\Gamma_i(s)$  is then taken as

$$W_T(s) = \frac{6\pi}{s + 6\pi}. \quad (20)$$

The filter frequency is set at 3 Hz such that the -3 dB point is not too close to the desired tracking frequency. We emphasize that, if a controller design is found with a gain higher than 0 dB, the system is not strictly string stable. For finite platoons this will not be a problem. This way a designer can trade-off disturbance rejection versus tracking performance.

##### B. Design of $W_u(s)$

The weight on the control action is chosen as the inverse of the steering dynamics given in (2). The steering dynamics attenuate high-frequency signals. For this reason, it is desired that the steering reference is generated in such a manner that it does not contain high-frequency components. The weight is given by

$$W_u(s) = \frac{s^2 + \zeta\omega_n s + \omega_n^2}{\omega_n^2 (s + 200\pi)(s + 201\pi)}, \quad (21)$$

where the two poles are required to make the transfer function proper.

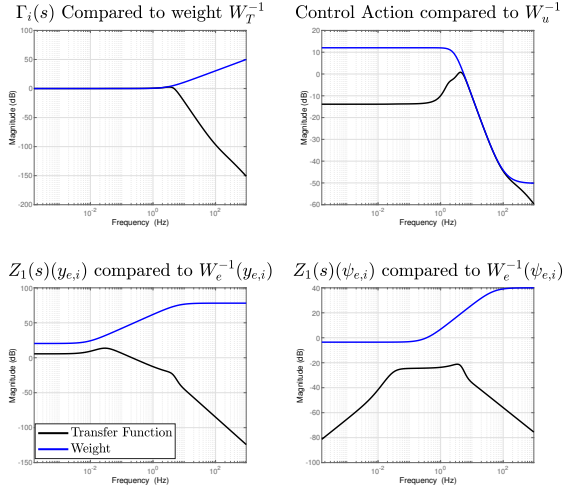


Fig. 5. Bode diagrams of the transfer functions compared to their weights. Top left shows the comparison between  $\Gamma_i(s)$  and its weight  $W_T$ . Top right shows the comparison between  $Z_3(s)$  and its weight  $W_u$ . The bottom left and right shows the comparison for the weight  $W_e$  on  $Z_1(s)$ .

### C. Design of $W_e(s)$

The design of the error weights is based on the allowable steady-state error. The average turn radius on a Dutch highway is around 750 metres [15]. If this is navigated at a velocity of 80 km/h, the vehicle has a yaw-rate of approximately 0.03 rad/s. Using (17), the DC-gain of the transfer functions can be used to directly convert the yaw rate of the preceding vehicle to a steady-state error.

From (15b) we see that a steady-state error in  $\psi_{e,i}$  results in an undesired accumulation of  $y_{e,i}$ . Therefore the synthesized controller should achieve zero steady-state error in  $\psi_{e,i}$ , which is already enforced by (20). Nevertheless a weight has to be included in the optimization. The weight used is given by

$$W_e(2, 2) = \frac{3 + 0.01s}{2 + s}.$$

For the lateral offset  $y_{e,i}$ , the maximum allowable steady-state offset is set at 30 cm, approximately a tyre's width. The maximum expected yaw rate is 0.03 rad/s. If transfer function (17) has a DC gain of 20 dB it means that, in steady-state, this yaw rate will be amplified by a factor of 10 to an output,  $y_{e,i}$ , of 0.3 m. Hence the weight has a DC gain close to 20 dB, where the final value is down to fine-tuning. The weight is, hence, chosen as

$$W_e(1, 1) = \frac{0.0075s + 0.3}{60s + \pi}.$$

### D. Synthesis Results

Fig. 5 shows the transfer functions given in (17), (18) and (19) and compares those to the related weight. The steady-state errors on both error states are within bounds, where  $\psi_{e,i}$  will have zero steady-state error. The limiting factor in controller synthesis are both the string stability and control action requirement.

Closer inspection of the graph showing  $W_T$  and its transfer function shows that  $\|\Gamma_i\|_\infty = 1.06$ . Strictly speaking, the system is not string stable but within the simulation results it was found that the lateral overshoot is in the order of several centimeters for a 4-vehicle platoon which satisfies the bound set by weight  $W_e(1, 1)$ .

## V. SIMULATION RESULTS

The velocity used in the simulation is 80 km/h. The distance between the vehicles is calculated as in [11],  $d_i = r_i + h_i v_x$ , where  $r_i$  is the stand still distance, set to be 5 m. The headway time,  $h_i$ , is the time gap between vehicles, which is set to 1 s. Both the distance and headway time are based on [11]. Given this stand-still-distance, velocity and headway time, the following distance becomes  $d_i = 27.2$  m.

A platoon of 4 vehicles is used in the simulation. No longitudinal dynamics are considered, a constant longitudinal velocity of 80 km/h is used and the aforementioned following distance  $d_i = 27.2$  m.

The performance of the proposed controllers is benchmarked against the controllers in [5]. This is the current point following controller employed by TNO. The results depicted in Fig. 6 show that the new proposed controller outperforms the currently used solution. Although the benchmark controllers do end up on the correct path, they do so with severe amplification of the yaw-rate.

### A. Discussion

The results of the simulation shows that the point- and path-following methods can be united using this new vehicle following method. Furthermore, it is shown that this method outperforms current path-following controllers. Using the new control method, the vehicle following objectives are met with little to no path deviation in transient response. Nevertheless, as shown in the previous section, the system is not strictly string stable.

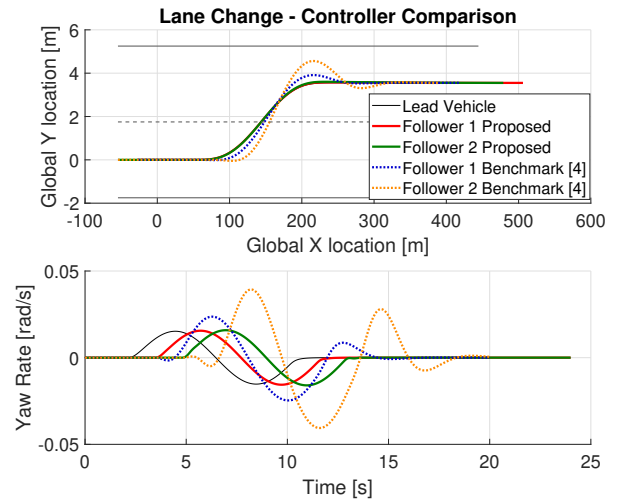


Fig. 6. Results of lane change simulation with a comparison between proposed controller, and the benchmark controller of [5].

To gain insight on the lateral overshoot that is caused by the disturbance amplification, we study at the transfer function from  $\theta_{s,i-1}$  to  $y_{e,i}$  in (17). It can provide insight in the amount of lateral error the vehicle will accumulate at a certain frequency. The input,  $\theta_{s,i-1}$ , is a signal with frequency of 0.1 Hz and a maximum amplitude of 0.015 rad/s. The amplification of (17) at 0.1 Hz, with this particular controller, is a factor of 2, meaning that at most the trailing vehicle will have an offset of 0.03 m which is well within the allowable bound. The 4<sup>th</sup> vehicle in the platoon will have an amplification of a factor  $2^4$  resulting in a maximum offset of 0.24 m, still within the steady-state error margin of weight  $W_e(2, 2)$ .

One of the ways to reduce the amount of lateral overshoot is to have a tighter restriction on the controller actuation. This can be achieved by reducing gain of weight  $W_u(s)$  over the entire frequency range. However, slowing down the controllers deteriorates the transient tracking performance which in turn could lead to dangerous situations.

Although this paper considers a system without delay, delay is expected to have negative impact on the string stability results similar to [3]. Having delay will also negatively impact the calculation of  $e_i(t) = y_{e,i}(t) + d_i\psi_{e,i}(t)$  at time  $t$  as it is dependant on  $\varepsilon_i(t)$ .

## VI. CONCLUSION

This paper presents a new vehicle following method. By using the positional information of the preceding vehicle, the road induced error can be calculated. Including this road error in the communication between two vehicles allows the trailing vehicle to deduce a compound distance error consisting of both positional and heading error. Using an observer it is further possible to reconstruct the individual road error states using the linear vehicle-road error model. The mathematical definition for string stability based on an infinity norm pairs well with an  $H_\infty$ -based controller. Using weights, it is possible to design controllers that minimize the disturbance amplification over the platoon. By finding the physical relation between the exogenous input and performance outputs, the weights can be designed in such a way that it gives a clear insight in the desired system performance. This makes the control design much more intuitive and gives the designer insight into how to tune his/her controller specific to a certain design scenario(s). It is shown using a theoretical analysis as well as simulations that the proposed vehicle following concept works well under normal highway driving conditions.

## REFERENCES

- [1] CBS. *Helpt meer kilometers dan in 1990*. Ed. by Unknown. 2019. URL: <https://www.cbs.nl/nl-nl-nieuws/2019/46/helpt-meer-kilometers-dan-in-1990> (visited on 02/13/2020).
- [2] C. Nieuwenhuizen Wijbenga. “RWS-2020/6225, 3e Rapportage Rijkswegennet 2019”. In: *2e Kamer Brief* (2020).
- [3] Jeroen Ploeg, Nathan van de Wouw, and Henk Nijmeijer. “Lp string stability of cascaded systems: Application to vehicle platooning”. In: *IEEE Transactions on Control Systems Technology* 22.2 (2013), pp. 786–793.
- [4] Michael P Lammert et al. “Effect of platooning on fuel consumption of class 8 vehicles over a range of speeds, following distances, and mass”. In: *SAE International Journal of Commercial Vehicles* 7.2014-01-2438 (2014), pp. 626–639.
- [5] Antoine Schmeitz et al. “Towards a generic lateral control concept for cooperative automated driving theoretical and experimental evaluation”. In: *2017 5th IEEE International Conference on Models and Technologies for Intelligent Transportation Systems (MT-ITS)*. IEEE. 2017, pp. 134–139.
- [6] Anggera Bayuwindra et al. “Combined lateral and longitudinal CACC for a unicycle-type platoon”. In: *2016 IEEE Intelligent Vehicles Symposium (IV)*. IEEE. 2016, pp. 527–532.
- [7] Federico Roselli et al. “ $H_\infty$  control with look-ahead for lane keeping in autonomous vehicles”. In: *2017 IEEE Conference on Control Technology and Applications (CCTA)*. IEEE. 2017, pp. 2220–2225.
- [8] Matteo Corno et al. “An LPV Approach to Autonomous Vehicle Path Tracking in the Presence of Steering Actuation Nonlinearities”. In: *IEEE Transactions on Control Systems Technology* (2020).
- [9] Daniel van den Berg. “A Lateral Control Solution for Cooperative Vehicle Platooning Applications”. In: *Tu Delft Master Thesis* (2020).
- [10] Omar Hassanain et al. “String-stable automated steering in cooperative driving applications”. In: *Vehicle System Dynamics* 58.5 (2020), pp. 826–842.
- [11] Jeroen Ploeg et al. “Design and experimental evaluation of cooperative adaptive cruise control”. In: *2011 14th International IEEE Conference on Intelligent Transportation Systems (ITSC)*. IEEE. 2011, pp. 260–265.
- [12] A.K. Saberi et al. “On functional safety methods: A system of systems approach”. In: *12th Annual IEEE International Systems Conference, SysCon 2018 - Proceedings*. 2018, pp. 1–6.
- [13] The MathWorks Inc. *Robust Control Toolbox*. Natick, Massachusetts, United States, 2021. URL: <https://nl.mathworks.com/products/robust.html>.
- [14] John R. McLean and Errol R. Hoffmann. “Analysis of Drivers Control Movements”. In: *Human Factors: The Journal of the Human Factors and Ergonomics Society* 13.5 (1971), pp. 407–418.
- [15] J. Vos. *Richtlijn Ontwerp Autosnelwegen 2017*. Tech. rep. Ministerie van Infrastructuur en Milieu, Nov. 27, 2017.